



Trends in air pollutants emissions in the Qinghai-Tibet Plateau and its surrounding areas under different socioeconomic scenarios[☆]

Ke Jiang^a, Ran Xing^a, Zhihan Luo^a, Jin Li^a, Yatai Men^a, Huizhong Shen^d, Guofeng Shen^{a,b,c,*}, Shu Tao^{a,b,d}

^a Laboratory for Earth Surface Processes, College of Urban and Environmental Sciences, Peking University, Beijing 100871, China

^b Institute of Carbon Neutrality, Peking University, Beijing 100871, China

^c School of Ecology and Environment, Zhengzhou University, Zhengzhou 45001, China

^d School of Environmental Sciences and Engineering, Southern University of Science and Technology, Shenzhen 518055, China



ARTICLE INFO

Editor: Hai Guo

Keywords:

Qinghai-Tibet Plateau
Air pollutants
Socioeconomic scenarios
Emission prediction

ABSTRACT

The Qinghai-Tibetan Plateau (QTP) and its surrounding areas are undergoing rapid changes in socioeconomic conditions, activity sectors, and emission levels. These changes underscore the significance of conducting local environmental assessments in the future and generating air pollutant emission forecasts necessary for effective evaluation. Current pollutants emissions pathways exhibit regional limitation since their based historical inventory could not accurately reflect the emission characteristics in QTP. This study constructed a high spatial resolution ($0.1^\circ \times 0.1^\circ$) atmospheric pollutant emissions dataset in the Qinghai-Tibet Plateau and its surrounding Areas (QTPA) based on updated emission inventory and various socioeconomic scenarios. We found that the pollutant emissions levels are distinct among different social development scenarios, with SSP3–7.0 demonstrating the highest magnitude of emissions. Regional and sectoral contributions exhibit substantial variations. Notably, solid fuel combustion originating from residential sectors in Northeast India and open fires in Myanmar are identified as high-density sources of PM_{2.5} emissions. Current pollutant emission patterns in the QTPA are more akin to SSP2–4.5, however, specific regions such as Qinghai and Tibet have exhibited more pronounced trends of emission reduction. The comparison with previous datasets reveals that the predicted pollutant emissions in this study are lower than Scenario Model Intercomparison Project (SMIP) dataset but higher than Asian-Pacific Integrated Model (AIM) dataset due to the revised inventory data and model variations, in which the latter might be the main obstacle to accurate emissions prediction.

1. Introduction

The Qinghai-Tibet Plateau (QTP) area, known for its highest mountains, largest glaciers, and most unique ecosystems in the world, is also one of the most vulnerable areas to environmental degradation and pollution (Chen et al., 2013). Atmospheric pollutants in the QTP have attracted more and more attention for their substantial impacts on ecological environment and human health (Ni et al., 2016; Jin et al., 2022). For instance, black carbon is regarded as an important short-lived climate pollutant (SLCP) affecting regional temperature and hydrological transformation in the QTP, which subsequently promoted the melting of glaciers (Li et al., 2016). Short-lived particle and gaseous pollutants from surrounding areas could be carried into the QTP through

the transboundary transport, inducing an undeniable influence on the air quality of the pure plateau. (Sierra-Hernández et al., 2019; Yang et al., 2020). Relatively high levels of fine particulate matters (PM_{2.5}) formed from primary carbonaceous aerosols and gaseous precursors have been observed in several cities of QTP, such as Lhasa and Xining, posing increasing exposure risks to the population in this area (Wu et al., 2018; Li et al., 2019).

The socioeconomic conditions, activity sectors, and emission levels in the QTP and its surrounding areas are currently undergoing rapid changes. This highlights the importance of evaluating the climate impacts, air quality, and health risks associated with atmospheric pollutants in the future, which relies on the establishment and prediction of an applicable emission inventory under diverse socioeconomic scenarios.

[☆] Notes: The authors declare no competing financial interest.

* Corresponding author at: Laboratory for Earth Surface Processes, College of Urban and Environmental Sciences, Peking University, Beijing 100871, China.

E-mail address: gfschen12@pku.edu.cn (G. Shen).

Furthermore, it is essential to explore regional and sectoral emission characteristics to identify effective mitigation measures. The Representative Concentration Pathways (RCPs) and Shared Socioeconomic Pathways (SSPs) are two representative scenario clusters (Van Vuuren et al., 2011; Riahi et al., 2017), and the emission pathways constructed in those have been applied to the fifth and sixth assessment report (AR5 and AR6) of Intergovernmental Panel on Climate Change (IPCC) (IPCC, 2013; IPCC, 2021). SSPs combines socioeconomic factors and climate goals in RCPs to construct a complete scenario set, providing the latest foundational inventory for studying future pollution and climate change in the Coupled Model Intercomparison Project phase 6 (CMIP6). (Gidden et al., 2019)

RCPs and SSPs play an irreplaceable role in global-scale climate change research (Huang et al., 2016; Rogelj et al., 2018), however, they may have certain limitations in studies at regional and local scales. As selecting Emissions Database for Global Atmospheric Research (EDGAR) and Community Emissions Data System (CEDS) as the driver emissions, SSPs inherit some limitations in these two inventories, e.g. air pollutant emission factors, sectoral activity intensity, and spatial interpolation factors, especially for typical air pollutants in the QTP and surrounding areas, may be biased and lagged (Hoesly et al., 2018; Crippa et al., 2020; Gidden et al., 2019). Large amounts of solid fuels were burned in this region, however, not accurately accounted in most statistics. Luo et al. (2020) points out the less reliability of CEDS in the simulation and validation of SO₂ pollution in Asia and China (Luo et al., 2020). Kanaya et al. (2020) highlighted that CEDS has not caught the rapid reduction of black carbon emissions in China since 2010 (Kanaya et al., 2020). Moreover, a comparative study by Xu et al. (2021) found substantial uncertainties between CEDS and EDGAR regarding BC emissions (Xu et al., 2021). Future air pollutant emissions dataset based on updated and more accurate spatially-resolved emission inventory is needed for QTP and its surrounding areas to conduct more effective scenario assessment.

In this study, based on our updated emission inventory and the emission pathways in different SSPs scenarios, we constructed a high spatial resolution ($0.1^\circ \times 0.1^\circ$) atmospheric pollutant emissions dataset in the Qinghai-Tibet Plateau and its surrounding Area (QTPA), which consists of two Chinese province, Qinghai and Tibet, and six countries around the QTP: India (IND), Pakistan (PAK) Bangladesh (BGD) Nepal (NPL), Bhutan (BTN), and Myanmar (MMR). The regional, sectoral and temporal emission characteristics for each air pollutant were analyzed under different scenarios, and results were compared to some previous scenario datasets.

2. Data and method

2.1. Emission data for the baseline year and under future scenarios

Historical pollutant emissions for all the countries in this study, including black carbon (BC), organic carbon (OC), fine particulate matters (PM_{2.5}), nitrogen oxides (NO_x), sulfur dioxide (SO₂) and carbon monoxide (CO), were derived from PKU inventory which adopted a bottom-up method to attributed emissions to 88 specific sectors and covered 224 countries and regions worldwide. The inventory included detailed energy structure survey results for the country including the Qinghai-Tibet Plateau (Tao et al., 2018; Jiao et al., 2023), that were thought to accurately capture the consumption data of non-commercial solid fuels in home, which is a major source of regional air pollutant emissions. Other information, including emission factories (EFs) and controlling technologies are also gathered from first-hand national and regional surveys, filed measurements (Shen et al., 2020; Liu et al., 2021) and literature values especially those on local emissions (Lu et al., 2011; Wang et al., 2014), making it more convincible of application in QTPA. The inventory has been applied for multiple regional air quality simulations, and the comparison with observations and results from other inventories validates the reliability of PKU inventory in the Asian region

(Shen et al., 2019; Luo et al., 2020). The national pollutant emissions in 2015 was utilized as the driver data in the base year of future scenarios, and historical emissions from 2000 to 2015 were accessed to compare the temporal emission change trends at website <http://inventory.pku.edu.cn>.

We adopted the framework of shared socioeconomic pathways (SSPs) as the basic of the prediction of future pollutant emissions in this study. Considering both socioeconomic dimensions and climate targets, the SSPs depicted the different future outcome including energy structure, land use change, GHGs and air pollutants emissions through various Integrated Assessment Models (IAMs). IPCC AR6 selected five representative SSPs scenarios to simulate the future earth system change, including SSP1–1.9, SSP1–2.6, SSP2–4.5, SSP3–7.0 and SSP5–8.5, which were also applied to this study. The first serial numbers (SSP1–SSP5) represent different socioeconomic development scenarios, when the following number (1.9–8.5) indicate the radiative forcing targets ($\text{W}\cdot\text{m}^{-2}$) at the end of the 21th century. The construction and model quantifications have been detailed in a series of literature (O'Neill et al., 2016; Riahi et al., 2017; Bauer et al., 2017; Popp et al., 2017; Rao et al., 2017), and the outcome data are available in <https://tntcat.iiasa.ac.at/SspDb>, where the pollutant emissions including BC, OC, NO_x, SO₂, and CO from nine sectors (detailed in Table S1) under the five SSPs scenarios in regional scales were accessed, along with future national gross domestic product (GDP) prediction used for downscaling. Due to similar emission characteristic between SSP1–1.9 and SSP1–2.6, this study focused on the analysis of the later four scenarios (SSP1–2.6 to SSP5–8.5).

2.2. Harmonization of future emissions through the base-year dataset

Due to the differences between the historical emissions datasets used for different SSPs scenarios and IAMs, as well as their areas accuracy and representativeness in the QTP, there may exist significant biases in the pollutant emission pathways constructed by the current framework of Scenario Model Intercomparison Project (SMIP). As a consequence, we first adopted the harmonization method promoted by Gidden et al. (2019) to harmonize the regional pollutant emissions consistent with the base-year dataset from PKU inventory in this study (Gidden et al., 2019).

The study areas are distributed in a total of 18 regions divided by different IAMs which are adapted to different scenarios simulation, and the detailed regional division information is shown in Table S2. For each region mentioned and each emission sector, pollutant emissions trajectory from SSPs database was harmonized to ensure the consistency between its initial point and PKU inventory in base year 2015. The harmonization processes were conducted by the available open-source software Aneris developed by Gidden et al. (Gidden, 2017; Gidden et al., 2018), which could choose different harmonizing methods based on the behaviour of emissions trajectory, as well as its difference from historical emissions, including ratio methods and offset methods, detailed in <http://mattgidden.com/aneris>.

2.3. Downscaling to country and grid level

This study adopted the convergency method being primarily proposed by van Vuuren et al. (2007) to downscale the regional pollutant emissions to national scale based on GDP prediction data. The emissions related to land use change and open burning (AFOLU) are downscaled with the linear method due to their low correlation to economy:

$$E_{c,s,p}^{PKU}(t) = E_{c,s,p}^{PKU}(t_0)^* \frac{E_{r,s,p}^{SSP}(t)}{E_{r,s,p}^{SSP}(t_0)} \quad t \in [2015, 2100]$$

where $E_{c,s,p}^{PKU}(t)$ represents the emission prediction in year t in this study; c is the country; s in the sector, p is the pollutant, when $E_{c,s,p}^{PKU}(t_0)$ is the emission from PKU inventory in base year t_0 ($t_0 = 2015$). The $E_{r,s,p}^{SSP}(t)$

represents the harmonized emission simulated in the specific SSP scenario and IAM, in which r is the region (divided by IAM) containing the country c , and $E_{r,s,p}^{SSP}(t_0)$ is the emission adopted by the IAM as the driver inventory (e.g., CEDS) in t_0 .

For other anthropogenic sectors, the emissions were downscale to country scale through converging national sectoral GDP-emission factor from the base year t_0 to the convergency year t_1 ($t_1 = 2100$). First, in the base year, the national GDP-emission factor is defined as:

$$F_{c,s,p}^{PKU}(t_0) = \frac{E_{c,s,p}^{PKU}(t_0)}{GDP_c(t_0)}$$

and for the region r containing the country c , this factor could be calculated by harmonized regional emission in t_1 :

$$F_{r,s,p}^{SSP}(t_1) = \frac{E_{r,s,p}^{SSP}(t_1)}{GDP_r(t_1)}$$

The convergency of nation GDP-emission factor could be described by the following equation:

$$F_{c,s,p}^{PKU}(t) = F_{c,s,p}^{PKU}(t_0) \times \left(\frac{F_{r,s,p}^{SSP}(t_1)}{F_{c,s,p}^{PKU}(t_0)} \right)^{\frac{t-t_0}{t_1-t_0}} \quad t \in [2015, 2100]$$

and the predicted national emission is subsequently calculated by:

$$\tilde{E}_{c,s,p}^{PKU}(t) = F_{c,s,p}^{PKU}(t) \times GDP_c(t)$$

To make sure the sum of emissions from all countries within the region is equal to the harmonized regional emission, the national emission was normalized as the final output:

$$E_{c,s,p}^{PKU}(t) = \tilde{E}_{c,s,p}^{PKU}(t) \times \frac{\sum_{c_i \in r} \tilde{E}_{c_i,s,p}^{PKU}(t)}{\sum_{c_i \in r} \tilde{E}_{c_i,s,p}^{PKU}(t)}$$

PKU inventory downscaled the national emissions to $0.1^\circ \times 0.1^\circ$ grid

level by different sectors, where various proxies of activity levels were considered, such as population density, power plant location and GDP (Xu et al., 2021). In this study, we assumed the consistency in the proportion of grid sectoral emission levels in the future, and conducted the grid downscaling for all the countries in this study according to the national sectoral emission distribution in the base year. The grids emissions from Qinghai and Tibet were summarized by the grids downscaled from China.

2.4. Primary PM_{2.5} emission prediction

PKU inventory conducted the global quantification of primary PM_{2.5} emissions that have not been simulated in the SSPs scenarios (Huang et al., 2014). BC and OC are important components of primary PM_{2.5}, and their emissions exhibit a significant correlation (Wu et al., 2016). For each country and sector, we constructed a linear regression equation between PM_{2.5} emissions and BC (or OC, decided by R²) emissions through historical inventory from 1960 to 2014, when the slope, intercept and R² are shown in Table S3. Based on the regression equations, national PM_{2.5} emissions were predicted under different scenarios, and downscaled to grid level as the method mentioned above.

3. Result and discussion

3.1. Predicted pollutant emissions in QTPA by 2060

The population, energy utilization, industry technology, and emissions of greenhouse gases and pollutants are distinct in different socio-economic scenarios. The midway year 2060 was selected to describe the emission characteristics, when Fig. 1 shows the predicted emissions of targeted air pollutants in the QTPA under different socioeconomic scenarios. Current BC emission is about 1.1 Mt./yr (Xu et al., 2021), when SSP1-2.6 and SSP5-8.5 depict a substantial emission reduction by 2060, at 0.35 and 0.41 Mt./yr, respectively. SSP3-7.0 is the scenario equipped with weak policy strength and makes slow progress in pollution control

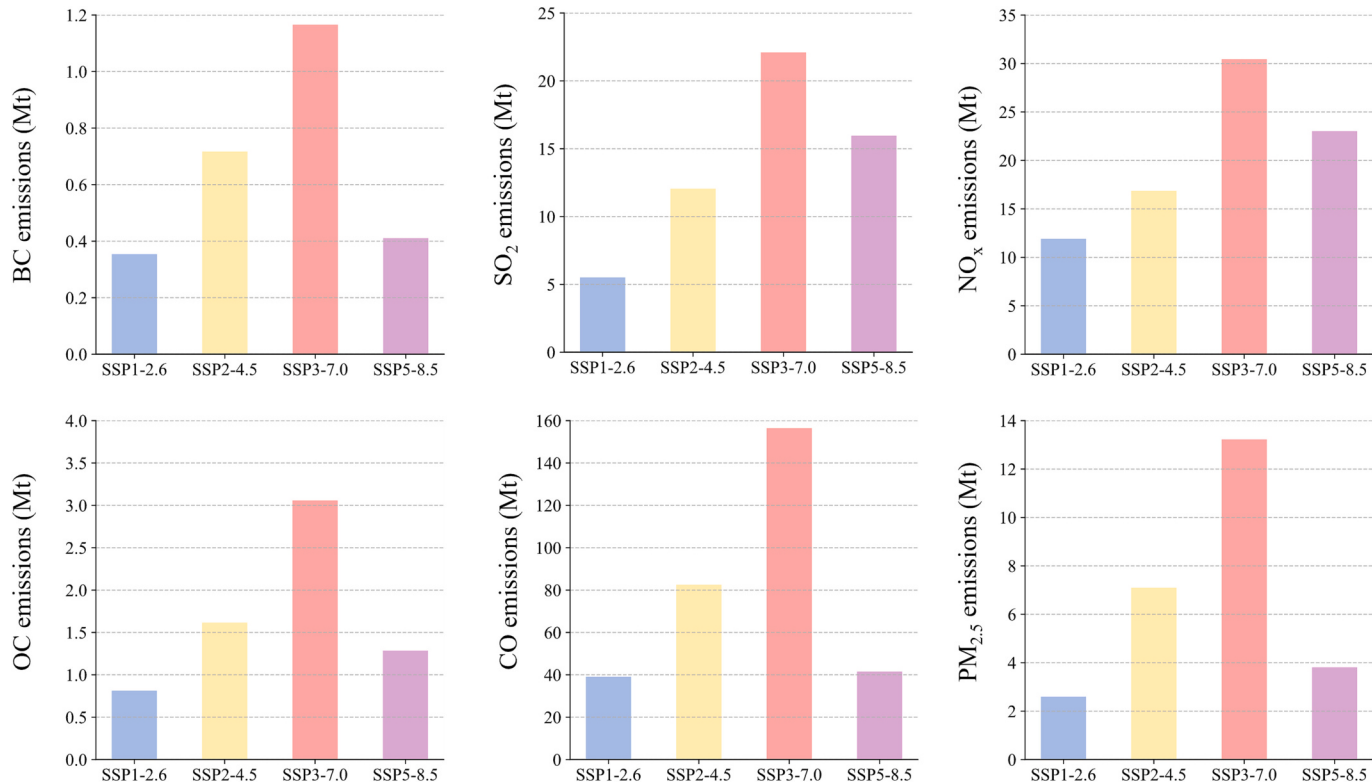


Fig. 1. Predicted emissions of different pollutants in QTPA under different socioeconomic scenarios in 2060.

(Rao et al., 2017), in which the QTPA expectedly emits enormous carbonaceous aerosols, resulting in the highest BC emission among all scenarios (1.17 Mt./yr), that was even higher than the current emission. The SO₂ and NO_x emissions under various scenarios have the same sort, with SSP3–7.0 the highest and SSP1–2.6 the lowest. The emissions of SO₂ range from 6 to 22 Mt./yr under different scenarios, when NO_x emissions range from 12 to 30 Mt./yr. However, different from the BC, SSP5–8.5 has the higher emissions of these two gases than SSP2–4.5 due to their different source contributions. Under various scenarios, the emission trends of OC, CO, and PM_{2.5} are similar to that of BC, suggesting that these pollutants exhibit analogous emission trends within a given socio-economic situation, contingent upon multifaceted factors encompassing energy utilization, policy, and technology.

Besides the total amount and its trend in the QTPA, it is more concerned in the spatial distribution of air pollutant emissions in the regions. Fig. 2 shows the gridded PM_{2.5} emission density under different scenarios in 2060, with the specific pollutant emissions in each country/province shown in Fig. S1. The PM_{2.5} emissions in Myanmar exhibit relative consistency (~0.5 Mt./yr) across diverse scenarios. India contributed most of the pollutant emissions in the QTPA, from 63 % (SSP1–2.6) to 82 % (SSP3–7.0) in total PM_{2.5} emissions. Among the six pollutants in the QTPA, SO₂ has the highest contribution from India, accounting for approximately 90 % in all scenarios. Like other pollutants, SSP3–7.0 is the scenario with the highest emissions of PM_{2.5} in India, at 11 Mt./yr, where the intense pollution emissions in Northeast India are mainly from the combustion of residential solid fuels, possibly having significant impacts on air quality in the Qinghai-Tibet Plateau through the transport and migration process (Yang et al., 2021). Similar

with PM_{2.5}, other pollutants are also emitted at high concentrations in Northeast India and north western Myanmar as shown in Figs. S2–S6, owing mostly to the residential sector and open fire. Despite the wide area, Qinghai and Tibet province exhibit relatively low levels of pollutant emission in both present-day and future scenarios. The total PM_{2.5} emissions of the two provinces do no exceed 140 Gg/yr under any scenario, with the contribution from 1.0 % (SSP3–7.0) to 2.8 % (SSP5–8.5) of total emissions in the QTPA. Pakistan and Bangladesh are significant pollutant contributors due to their large population (Liu et al., 2022), and exhibit similar emission trends among different scenarios for the same pollutant, being mainly induced by their similar energy structure and technologic levels.

3.2. Sectoral contributions to pollutant emissions under different scenarios

Fig. 3 shows the contribution of different sectors to pollutant emissions in the QTPA, with obvious variations under different socioeconomic pathways. Among the scenarios considered, SSP5–8.5 exhibits the greatest influence of AFOLU on most pollutant emissions, especially for OC, which account for 72 % of total emissions. This could mainly be attributed to the feedback of terrestrial ecosystems triggered by strong climate change, leading to the frequent occurrence of wildfires (Scholze et al., 2006). In the context of this heavily fossil fuel-reliant scenario, emissions of BC and PM_{2.5} are predominantly from oil burned in transport and coal burned in power plants, generating 45 % and 43 % of total emissions, respectively. Anthropogenic activities dominate the pollutant emissions in SSP2–4.5 and SSP3–7.0 due to the insufficient carbon and

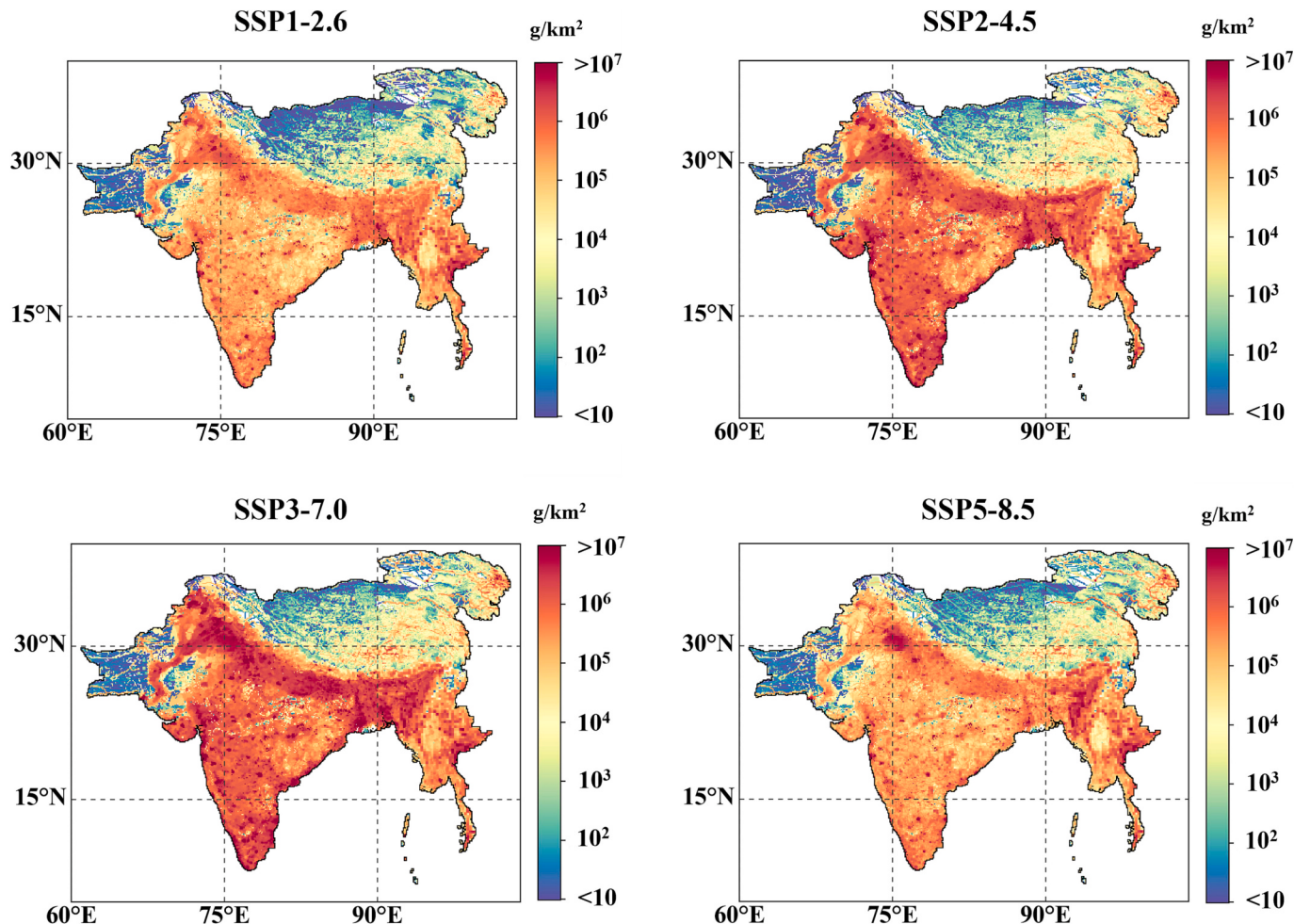


Fig. 2. The gridded emission density of PM_{2.5} in study area under different socioeconomic scenarios in 2060.

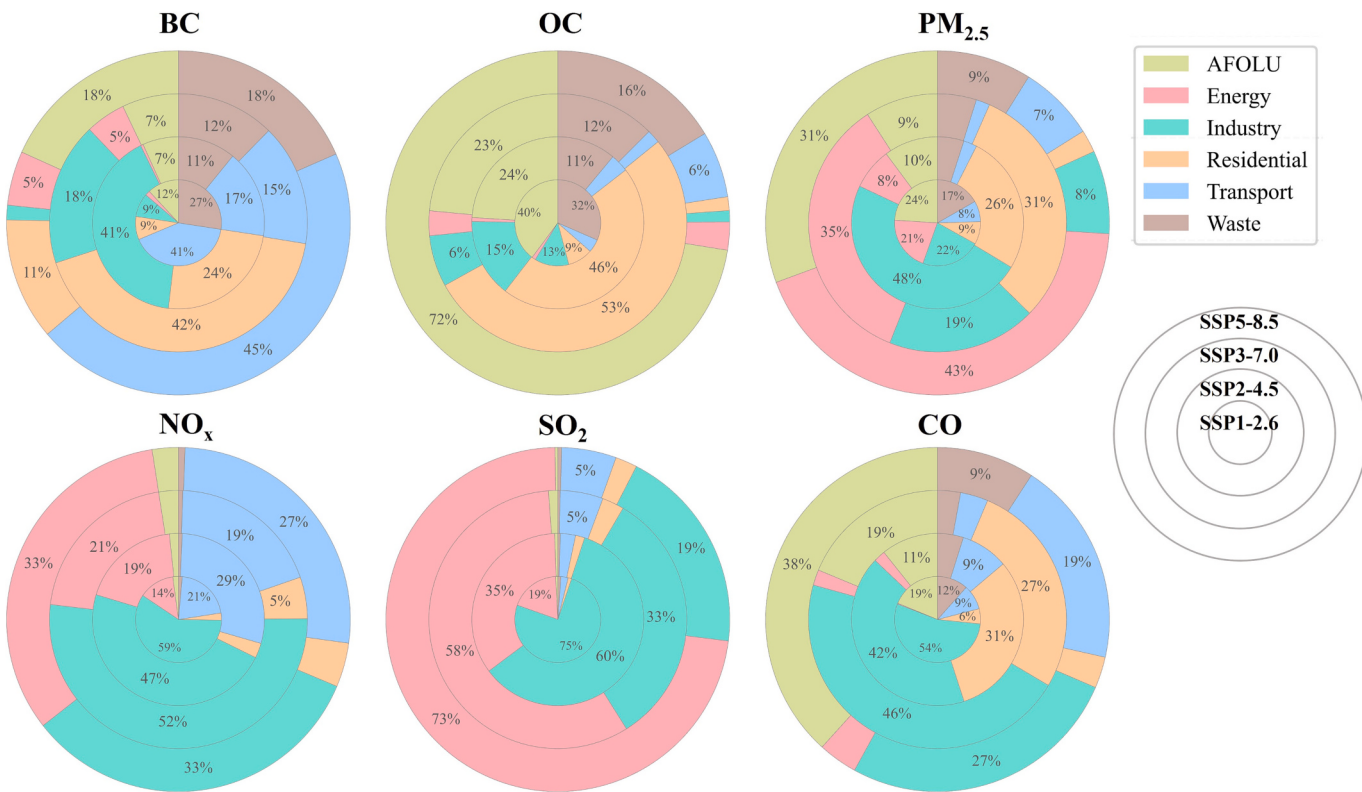


Fig. 3. The contribution of different sectors to pollutant emissions in QTPA under different socioeconomic scenarios in 2060.

pollution controls. For BC, OC and PM_{2.5}, residential and industrial activities contribute the majority of emissions in SSP2–4.5 and SSP3–7.0, when energy sector and AFOLU also exhibit considerable contribution in specific pollutant and scenario. SSP1–2.6 adopted strong and effective mitigation policies and technologies, in which large amounts of emissions would be from the waste combustion after effective controls on pollutant emissions from other energy utilization activities (van Vuuren et al., 2017). This underscores the importance of addressing waste management practices as a key component in mitigating air pollution and achieving sustainable development.

Energy, industry, and transport are the large sectors responsible for NO_x emissions, although the contribution shares vary across scenarios. In SSP5–8.5, the contributions of these three sectors are approximately equal at around 30 %, whereas industrial activities dominate emissions in other scenarios. SO₂ emissions are largely attributed to the energy and industry sectors, which collectively account for over 90 % of all emissions across each scenario. Notably, there is a significant shift in the contribution of these sectors to SO₂ emissions from the SSP1–2.6 to SSP5–8.5 scenarios, with the energy sector's contribution steadily increasing from 19 % to 73 %, while the industry sector's contribution subsequently decreases from 75 % to 19 %. This could be partly explained by variation of coal consumption and industry technologies among different scenarios. With the exception of SSP5–8.5, the industry sector is the largest contributor to CO emissions across all scenarios. In addition, incomplete biomass burning in the AFOLU and residential sectors results in a significant proportion of CO emissions in specific scenarios.

The largest sector of BC emission on the grid level is shown in Fig. 4, and the national sectoral contributions are illustrated in Fig. S7. In most areas of Myanmar, the AFOLU is the primary sector of BC emissions under all scenarios, with the contribution ranging from 77 % in SSP3–7.0 to 94 % in SSP2–4.5. The dominant sector in other areas varies by scenarios. In SSP2–4.6, industrial activities dominate the BC emissions in most grids of India, while in northeastern India residential fuel

combustion emissions are still predominant. Residential source is also the most substantial BC emission sectors in most parts of Tibet and South Asia in SSP3–7.0. Waste disposal would have a unignorable contribution to the BC emission in SSP1–2.6, accounting for 34 % and 51 % in Qinghai and Tibet, respectively. Transportation also dominates the BC emissions in India and Pakistan, which is more evident in SSP1–2.6 and SSP5–8.5, contributing to 44 % of Indian emissions and >50 % of Pakistani emissions. Despite the low contribution, BC emissions from energy sector are concentrated at several factory point sources, and dominate in these grids. Figs. S8–S12 illustrate the grid dominant sector for other pollutants. The spatial distributions of OC and PM_{2.5} emission sector are generally consistent with BC, while residential and industrial source exhibit more significant contribution to Indian OC emissions in SSP2–4.5 and PM_{2.5} emissions in SSP1–2.6, respectively. Different with particulates, industry dominates the emissions of gaseous pollutants in most grids of QTPA in each scenario. Transportation also covers considerable NO_x emission grids, expressed as the traffic route shape, when energy sector contributes substantial SO₂ emissions in north-eastern India in SSP3–7.0 and SSP5–8.5.

3.3. Distinct time-series in pollutant emissions

Fig. 5 shows the temporal emissions of targeted air pollutants in the study area under different scenarios, when the real-world emissions from 2015 to 2019 are also illustrated as a comparison. BC, OC and PM_{2.5} have similar trends, as their emissions undergo a swift reduction owing to pollution control measures implemented in the ambient target scenarios SSP1–1.9 and SSP1–2.6. Their emissions display diverse degrees of increasing trend, primarily attributed to the industry sector, before 2030 in SSP2–4.5 and 2050 in SSP3–7.0, and then subsequently decline to different levels by 2100. In SSP5–8.5, these three pollutants also decrease rapidly before 2050 due to the development and cleanliness of fossil fuels, and then, BC and PM_{2.5} emissions still exhibit the slow downward trend, however, there would still an increase in OC

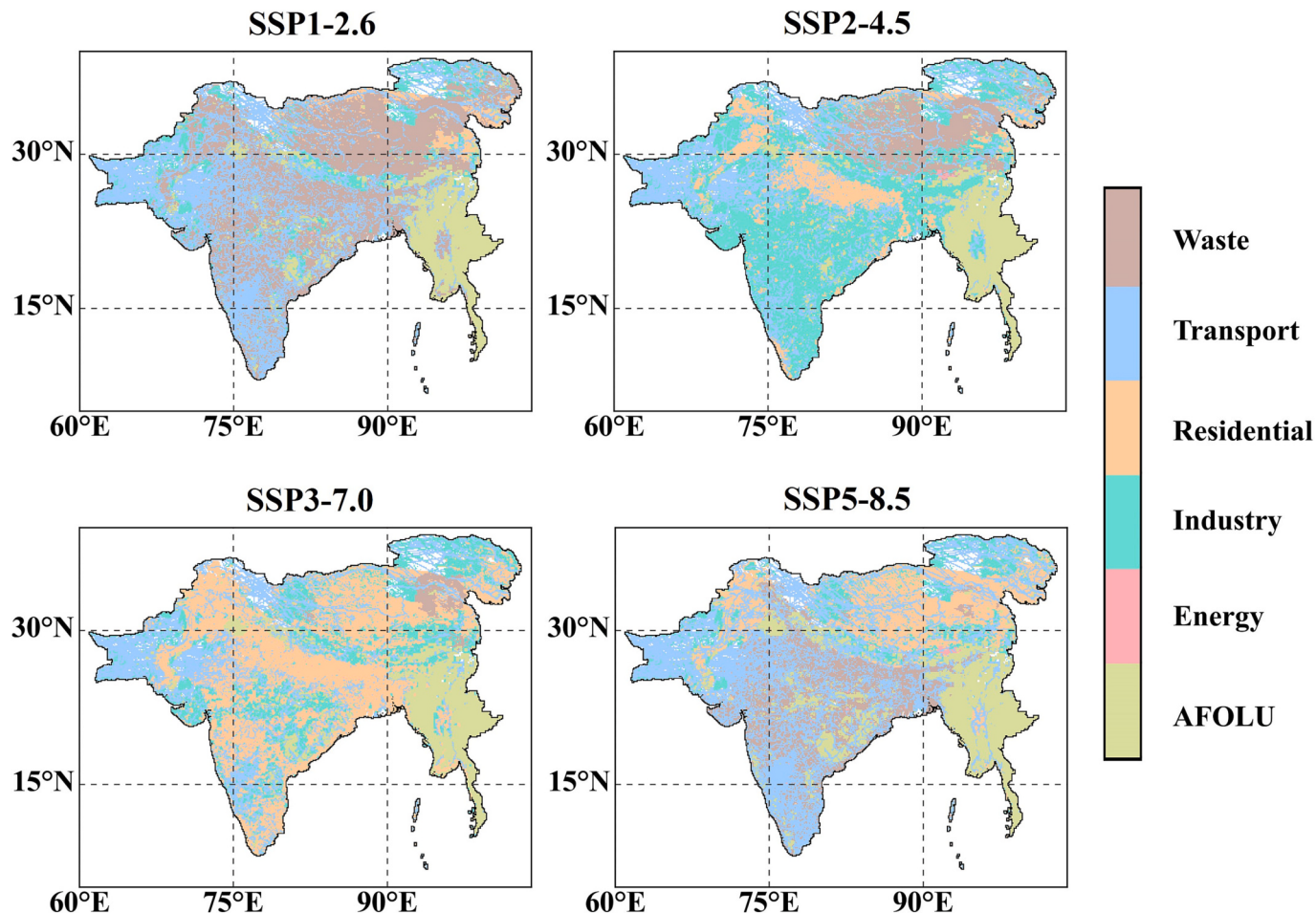


Fig. 4. The sector with predominant contribution of BC emissions in QTPA under different socioeconomic scenarios in 2060.

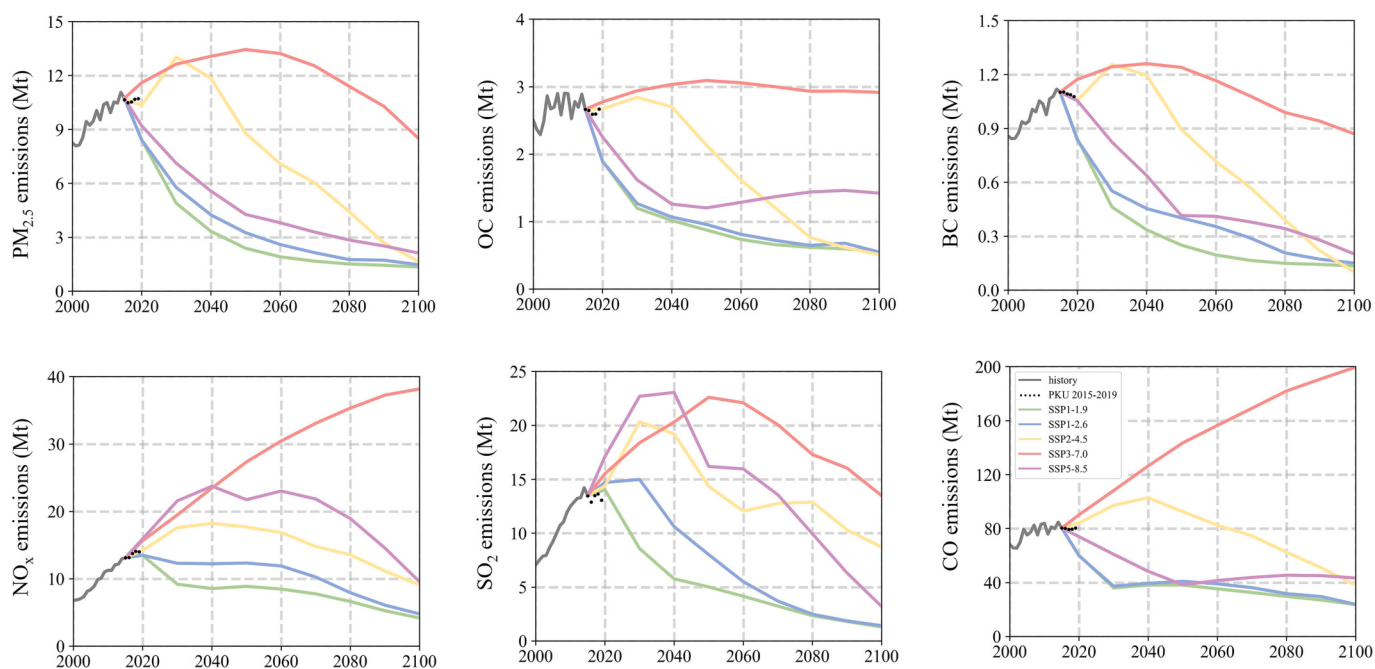


Fig. 5. The temporal trend of different pollutant emissions in QTPA under different scenarios (color line), and the comparison with PKU inventory between 2015 and 2019 (dot).

emissions, mainly derived from the frequent biomass burning under intense climate change on the road leading to 8.5 W/m^2 .

In the most polluted SSP3–7.0, NO_x and CO emissions increase continuously to 38 Mt./yr and 200 Mt./yr in 2100, that were about 2-fold larger than their emissions in 2015, when SO_2 emissions peak at 23 Mt./yr in 2050 and gradually decrease to 13 Mt./yr in 2100. The mitigation degree of NO_x and CO in SSP1–1.9 and SSP1–2.6 is also weaker than that of carbonaceous pollutants and SO_2 , which implicates it difficult to control these two pollutants and the ozone pollution related to them should be given sufficient attention in the future. (Ran et al., 2014) Different from carbonaceous pollutants, NO_x and SO_2 emissions in SSP5–8.5 continue the historical increasing trends until 2040, consistent with the rise in demand for energy from fossil fuels. (Kriegler et al., 2017)

From the perspective of current emissions, the trajectories of practically all pollutants from 2015 to 2019 are more akin to the middle of the road (SSP2–4.5), indicating that there has been no substantial transition in present society, economy, and technology compared with historical patterns. (Riahi et al., 2017) For example, after 2015, SO_2 emissions in the QTPA exhibit a fluctuating but generally declining trend, resembling the pattern of SSP1, which is primarily attributed to the potent industrial pollution control in China and South Asian countries (Lu et al., 2020). The construction of updated pathways is needed to guide the direction of further climate mitigation under the latest socioeconomic scenarios and emission status, and effective policies and measures should be considered to achieve ambitious climate goals such as SSP1–1.9 and SSP1–2.6.

Fig. 6 shows the temporal contribution of various sectors to $\text{PM}_{2.5}$ emissions in different scenarios. The residential emissions are the main pollution source in QTPA (Liu et al., 2022), accounting for 39 % of total $\text{PM}_{2.5}$ emissions in 2015, but the contribution would decrease rapidly under 10 % in SSP1–2.6 and SSP5–8.5. The AFOLU and waste disposal subsequently account for a higher proportion of $\text{PM}_{2.5}$ emissions due to the difficulty of reducing their emissions through mitigation policies. The contribution of energy sector in SSP5–8.5 will increase from 16 % in

2015 to 50 % in 2050, which is mainly because the electricity demands highly depend on fossil fuel combustion (especially coals), even resulting in the increase of the absolute $\text{PM}_{2.5}$ emission from energy sector despite the mitigation technologies. In SSP3–7.0, residential contribution does not show large fluctuations in time series, and maintains its value exceeding 30 %, while the industrial contribution would decrease continuously from 31 % in 2015 to 7 % in 2100. Differently, the industry may contribute more $\text{PM}_{2.5}$ emissions in SSP2–4.5 until 2080, when the residential emissions are reduced significantly.

Fig. S13 depicts the sectoral contributions of other pollutant emissions except $\text{PM}_{2.5}$, in time series. Similar with $\text{PM}_{2.5}$, residential sources would contribute significantly to BC and OC emissions in SSP3–7.0, as a consequence of the persistent and rapid population expansion. Under all scenarios, the contribution of AFOLU to OC emissions shows increasing trends, particularly for SSP5–8.5, which may be primarily attributable to anthropogenic mitigation and the increase in fires in the context of climate change. Owing to the utilization of sustainable and clean energy, industrial processes typically provide the majority of the gaseous pollutants in SSP1–2.6. The percentage of SO_2 and NO_x emissions from power plants also significantly reduces as coal consumption declines. Transportation produced a share of the NO_x emissions in SSP2–4.5 since the majority of vehicles still burn a lot of oil to generate energy.

Temporal trends in air pollutant emissions in some countries/regions are illustrated in Fig. S14, as well as the comparison with the emissions between 2015 and 2019. National sectoral contributions to $\text{PM}_{2.5}$ emissions in time series are shown in Fig. S15. Emissions of targeted air pollutants in this study experienced a rapid decrease in Qinghai and Tibet, whose trends are closer to SSP1–1.9 and SSP1–2.6 under clean energy transformation in China. Under this scenario, residential and open burning emissions would be the primary sectors contributing to $\text{PM}_{2.5}$ emissions in the plateau. India, Pakistan and Bangladesh have similar sectoral shares to $\text{PM}_{2.5}$ emissions under each scenario, and are large emitters in the QTPA. While SSP2–4.5 or SSP5–8.5 can precisely predict the pollutant emissions from 2015 to 2019 in India and

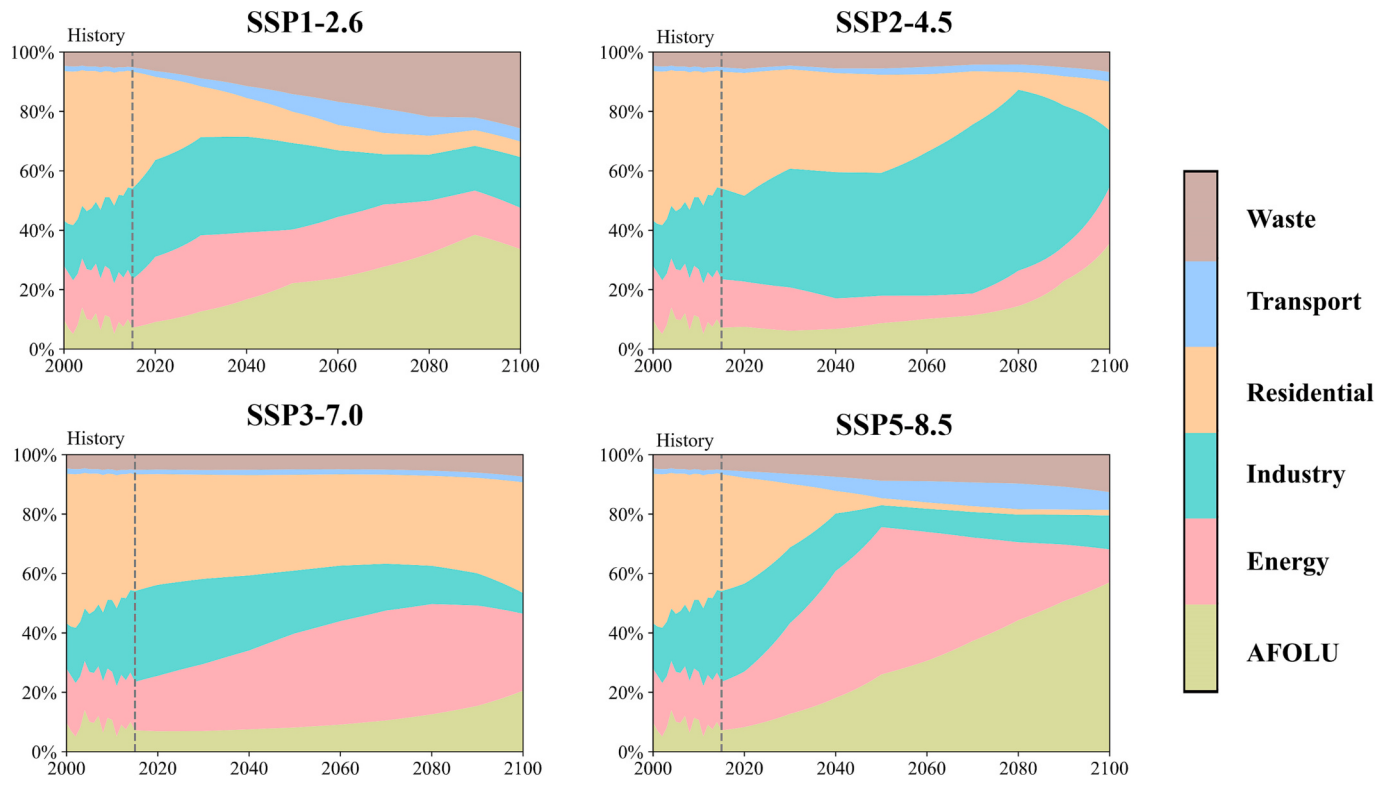


Fig. 6. The temporal contribution of different sectors to $\text{PM}_{2.5}$ emissions in QTPA under different scenarios.

Bangladesh, some pollutants like PM_{2.5}, OC, and CO in Pakistan continuously grow, and likely even exceed the most polluted scenario SSP3–7.0. This indicates that the IAM with higher spatial resolutions needs to be developed and applied to accurately simulate the national emissions (Tong et al., 2020). >60 % of current PM_{2.5} emissions in Myanmar were generated by AFOLU, and under all scenarios, this source would remain the largest emitter. SSPs primarily consider the pollutant mitigation on anthropogenic sectors, resulting in slight differences among different scenarios in Myanmar. Land use management and wildfire controls can be implemented in Myanmar to effectively decrease local air pollutant emissions in future.

3.4. Comparison with other predictions

From the perspective of socioeconomic scenarios, several previous studies have simulated the GHGs and pollutant emission pathway on the global or regional scales through various IAMs. Gidden et al. constructed the harmonized global emissions pathways under different socioeconomic scenarios, and downscaled it to gridded scale (Gidden et al., 2019), which is the important part of Scenario Model Intercomparison Project (SMIP). Besides, Fujimori et al. also constructed long-term gridded emissions dataset based on a single IAM, the Asian-Pacific Integrated Model (AIM) (Fujimori et al., 2018). The spatial resolution of both two datasets is 0.5° × 0.5°, at which scale the comparison between our prediction and these two emission datasets was conducted for BC and NO_x emissions as the representative of particulate and gaseous pollutants, as seen in Fig. 7 and Tables S4 and S5.

The BC emissions predicted by SMIP are generally comparable with this study ($R^2 = 0.57$), but exhibit higher values in most grids, especially in northeastern Tibet. This is thought to be attributed to the overestimation of Chinese BC emissions by the CEDS inventory (Xu et al., 2021). In comparison to our study, the higher Indian BC emissions in SMIP are primarily derived from the residential sector, and the differences could be traced back to the initial driver data from 2015. On the other hand, the BC emissions simulated by AIM are significantly lower than our prediction, as well as those of SMIP, especially in the industry and transportation sectors. This indicates that the effectiveness of pollutant mitigation measures and their impacts are more pronounced in the SSP2–4.5 simulated by AIM. These comparisons also highlight the substantial output variations among different IAM frameworks, which will have greater impacts on pathway predictions than the difference in basic datasets.

Similar to BC, the NO_x emissions predicted by our study is also lower

than the SMIP dataset but higher than the AIM dataset. Though from a trend perspective, grid data still exhibits sequential consistency in the comparison, the total NO_x emissions of QTPA are 44 % higher in the SMIP, mainly concentrating on transportation sector. However, several on-road emissions in Qinghai and Tibet province caught in this study are also shown as higher grids (blue grids) in map comparison (Fig. 7b). The estimate of NO_x emissions by AFOLU in the AIM dataset was higher than that in this study, resulting in some higher grids in this region. For most other grids, the NO_x emissions in the AIM dataset are significantly lower, where the total emissions only account for 13 % of this study.

3.5. Implication and limitation

In this study, we predicted air pollutant emissions around the Qinghai-Tibet Plateau and surrounding areas based on the updated emission inventories and socioeconomic scenarios. The intense differences of various pollutant emissions are manifested in different scenarios due to differences of and changes in energy structure and emission characteristics (Amann et al., 2013). The transition pathways in response to climate change will have a decisive impact on the air quality and environmental ecology around the QTP in the future. The synergistic promotion on the melting of glaciers will be generated in SSP3–7.0 in terms of temperature increase and albedo decrease induced by larger radiative forcing and higher BC emissions (~0.8 Mt./yr) than SSP1–2.6, respectively (Yang et al., 2015). Atmospheric transport from surrounding areas is the main source of air pollution in Qinghai-Tibet Plateau, but some local pollutant emissions may increase in some scenarios (Fig. S13) and consequently would pose health risks to local population, that should not be underappreciated.

In terms of driving datasets, we harmonized and downscaled the emission with the updated inventory and gridded data, corrected pollutant emissions from the SMIP dataset in QTPA and provided a pollutant dataset (including PM_{2.5}) with higher spatial resolution (0.1° × 0.1°), which better supports future air quality simulation and environmental health risks assessment around this cleanest area. However, owing to the availability of various IAMs, this study could only conduct the harmonization and calibration based on the existing output of different scenarios and IAMs. consequently, the constraint targets and response to emissions may not be well captured by our dataset despite the similar temporal trends. This study concentrated on short-lived particulate and gaseous pollutant emissions prediction, when greenhouse gases have not been considered for their relatively weak impact on the local areas. Moreover, the inventory adopted in this study has not

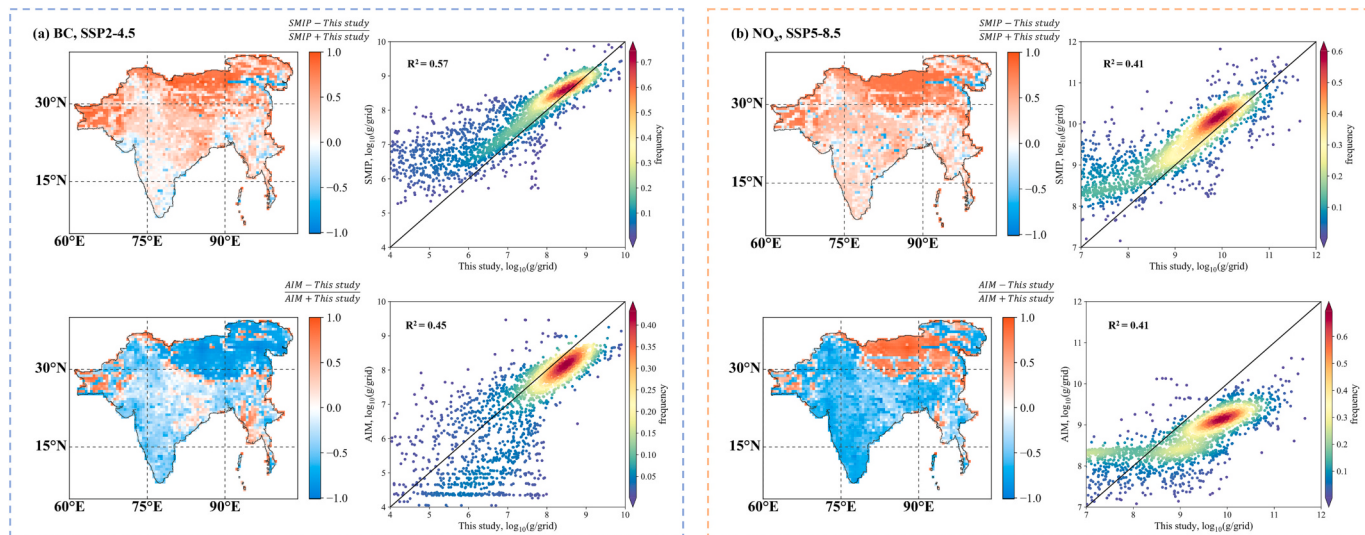


Fig. 7. Comparison of gridded (a) BC emissions in SSP2–4.5 and (b) NO_x emissions in SSP5–8.5 in 2060 between this study and SMIP dataset as well as AIM dataset.

made significant improvements in greenhouse gases emissions, whose predictions are primarily determined by the depiction of future scenarios.

The uncertainty of this study could stem from various aspects. First, there exists a certain initial uncertainty in the driver emission inventory based on the energy consumption and emission factors, which might be amplified during the scenario simulation. Second, multiple factors in the scenarios, including population increase, energy consumption and technology development (Cocks et al., 1998), will have a substantial influence on the uncertainty assessment, which could not be accomplished using only the fundamental driver data in this study. Moreover, the downscale technique does not account for the spatiotemporal variance of sectoral activity, resulting in higher grid-scale uncertainty. To remedy this issue, more plausible geographical scenarios need to be described. There still exists intense gap between the pollutant emissions in the same scenarios simulated by different IAMs, calling for more efforts needed to be invested in reconciling various models, constructing more accurate inventories, and reducing the uncertainties in pollutant emission pathways.

4. Conclusion

The study constructed new air pollutant emission datasets, including primary PM_{2.5}, OC, BC, CO, SO₂ and NO_x, with a high resolution of 0.1° × 0.1° in the QTPA under different socioeconomic scenarios based on the updated and more reliable inventories in the region. Sectoral and geographical contribution of pollutant emissions were thoroughly analyzed. The inventory adopted in this study addressed the constraints of EDGAR and CEDS in QTPA, yielding a lower result than the SMIP dataset but a higher result than the AIM dataset. Current pollutant emission patterns in the QTPA are more akin to SSP2–4.5, but there are substantial regional variabilities, with pollution mitigation in Qinghai and Tibet being more substantial and leaning to SSP1. The particulate emissions from the residential sector from northeastern India would be particularly substantial in SSP3–7.0, and might result in considerable impacts on the ecology and environment of the studied region. Open burning emissions should be highly concerned in Myanmar, requiring for special consideration in terms of land management and wildfire prevention.

CRediT authorship contribution statement

Ke Jiang: Formal analysis, Data curation, Writing – original draft. **Ran Xing:** Investigation, Data curation. **Zhihan Luo:** Writing – review & editing. **Jin Li:** Formal analysis, Data curation. **Yatai Men:** Formal analysis, Visualization. **Huizhong Shen:** Writing – review & editing. **Guofeng Shen:** Conceptualization, Writing – review & editing, Funding acquisition. **Shu Tao:** Supervision, Funding acquisition.

Declaration of competing interest

The authors declare that they have no known competing financial interests or personal relationships that could have appeared to influence the work reported in this paper.

Data availability

Data will be made available on request.

Acknowledgments

Funding for this study was provided by the Ministry of Science and Technology of China (2019QZKK0605) and National Natural Science Foundation (42077328).

Appendix A. Supplementary data

The following information associated with the text is provided and available online free of charge:

The sectoral and regional division; the regression equation to predict PM_{2.5} emission; the comparison with SMIP and AIM; the detail pollutant emissions by country/region; spatial distribution of emission density and dominant sector for each pollutant; temporal and sectoral trends of all pollutants emissions in all countries/regions under all scenarios. Supplementary data to this article can be found online at <https://doi.org/10.1016/j.scitotenv.2023.165745>.

References

- Amann, M., Klimont, Z., Wagner, F., 2013. Regional and global emissions of air pollutants: recent trends and future scenarios. *Annu. Rev. Environ. Resour.* 38, 31–55.
- Bauer, N., Calvin, K., Emmerling, J., Fricko, O., Fujimori, S., Hilaire, J., Eom, J., Krey, V., Kriegler, E., Mouratiadou, I., Sytze de Boer, H., van den Berg, M., Carrara, S., Daioglou, V., Drouet, L., Edmonds, J.E., Gernaat, D., Havlik, P., Johnson, N., Klein, D., Kyle, P., Marangoni, G., Masui, T., Pietzcker, R.C., Strubegger, M., Wise, M., Riahi, K., van Vuuren, D.P., 2017. Shared socio-economic pathways of the energy sector – quantifying the narratives. *Glob. Environ. Chang.* 42, 316–330.
- Chen, H., Zhu, Q., Peng, C., Wu, N., Wang, Y., Fang, X., Gao, Y., Zhu, D., Yang, G., Tian, J., Kang, X., Piao, S., Ouyang, H., Xiang, W., Luo, Z., Jiang, H., Song, X., Zhang, Y., Yu, G., Zhao, X., Gong, P., Yao, T., Wu, J., 2013. The impacts of climate change and human activities on biogeochemical cycles on the Qinghai-Tibetan Plateau. *Glob. Chang. Biol.* 19, 2940–2955.
- Cocks, A.T., Rodgers, I.R., Skeffington, R.A., Webb, A.H., 1998. The limitations of integrated assessment modelling in developing air pollution control policies. *Environ. Pollut.* 102, 635–639.
- Crippa, M., Solazzo, E., Huang, G., Guizzardi, D., Koffi, E., Muntean, M., Schieberle, C., Friedrich, R., Janssens-Maenhout, G., 2020. High resolution temporal profiles in the emissions database for global atmospheric research. *Sci. Data* 7, 121.
- Fujimori, S., Hasegawa, T., Ito, A., Takahashi, K., Masui, T., 2018. Gridded emissions and land-use data for 2005–2100 under diverse socioeconomic and climate mitigation scenarios. *Sci. Data* 5.
- Gidden, M.J., 2017. gidden/aneris: initial release version for harmonization paper (v0.1.0). Zenodo. <https://doi.org/10.5281/zenodo.802832>.
- Gidden, M.J., Fujimori, S., van den Berg, M., Klein, D., Smith, S.J., van Vuuren, D.P., Riahi, K., 2018. A methodology and implementation of automated emissions harmonization for use in integrated assessment models. *Environ. Model. Softw.* 105, 187–200.
- Gidden, M.J., Riahi, K., Smith, S.J., Fujimori, S., Luderer, G., Kriegler, E., van Vuuren, D.P., van den Berg, M., Feng, L., Klein, D., Calvin, K., Doelman, J.C., Frank, S., Fricko, O., Harmsen, M., Hasegawa, T., Havlik, P., Hilaire, J., Hoesly, R., Horing, J., Popp, A., Stehfest, E., Takahashi, K., 2019. Global emissions pathways under different socioeconomic scenarios for use in CMIP6: a dataset of harmonized emissions trajectories through the end of the century. *Geosci. Model Dev.* 12, 1443–1475.
- Hoesly, R.M., Smith, S.J., Feng, L.Y., Klimont, Z., Janssens-Maenhout, G., Pitkanen, T., Seibert, J.J., Vu, L., Andres, R.J., Bolt, R.M., Bond, T.C., Dawidowski, L., Khodol, N., Kurokawa, J., Li, M., Liu, L., Lu, Z.F., Moura, M.C.P., O'Rourke, P.R., Zhang, Q., 2018. Historical (1750–2014) anthropogenic emissions of reactive gases and aerosols from the community emissions data system (CEDS). *Geosci. Model Dev.* 11, 369–408.
- Huang, Y., Shen, H., Chen, H., Wang, R., Zhang, Y., Su, S., Chen, Y., Lin, N., Zhuo, S., Zhong, Q., Wang, X., Liu, J., Li, B., Liu, W., Tao, S., 2014. Quantification of global primary emissions of PM_{2.5}, PM₁₀, and TSP from combustion and industrial process sources. *Environ. Sci. Technol.* 48, 13834–13843.
- Huang, J.P., Yu, H.P., Guan, X.D., Wang, G.Y., Guo, R.X., 2016. Accelerated dryland expansion under climate change. *Nature. Climate Change* 6 (166–).
- IPCC, 2013. Climate Change 2013: The Physical Science Basis. Contribution of Working Group I to the Fifth Assessment Report of the Intergovernmental Panel on Climate Change. Cambridge University Press, Cambridge, United Kingdom and New York, NY, USA.
- IPCC, 2021. Climate Change 2021: The Physical Science Basis. Contribution of Working Group I to the Sixth Assessment Report of the Intergovernmental Panel on Climate Change. Cambridge University Press, Cambridge, United Kingdom and New York, NY, USA.
- Jiao, X., Xiong, R., Luo, Z., Li, Y., Cheng, H., Rashid, A., Shen, G., Tao, S., 2023. Household energy stacking and structures in Pakistan – results from a multiple-energy study in Azad Kashmir and Punjab. *J. Environ. Sci.* 133, 152–160.
- Jin, R., Zheng, M., Yang, L., Zhang, Q., Fu, J., Yang, R., Liu, Q., Shi, J., Liu, G., Jiang, G., 2022. Indoor exposure to products of incomplete combustion of household fuels in rural Tibetan Plateau. *Environ. Sci. Technol.* 56, 4711–4714.
- Kanaya, Y., Yamaji, K., Miyakawa, T., Taketani, F., Zhu, C., Choi, Y., Komazaki, Y., Ikeda, K., Kondo, Y., Klimont, Z., 2020. Rapid reduction in black carbon emissions from China: evidence from 2009–2019 observations on Fukue Island, Japan. *Atmos. Chem. Phys.* 20, 6339–6356.
- Kriegler, E., Bauer, N., Popp, A., Humpenöder, F., Leimbach, M., Streifler, J., Baumstark, L., Bodirsky, B.L., Hilaire, J., Klein, D., Mouratiadou, I., Weindl, I.,

- Bertram, C., Dietrich, J.-P., Luderer, G., Pehl, M., Pietzcker, R., Piontek, F., Lotze-Campen, H., Biewald, A., Bonsch, M., Giannousakis, A., Kreidenweis, U., Müller, C., Rolinski, S., Schultes, A., Schwanitz, J., Stevanovic, M., Calvin, K., Emmerling, J., Fujimori, S., Edenhofer, O., 2017. Fossil-fueled development (SSP5): an energy and resource intensive scenario for the 21st century. *Glob. Environ. Chang.* 42, 297–315.
- Li, C., Bosch, C., Kang, S., Andersson, A., Chen, P., Zhang, Q., Cong, Z., Chen, B., Qin, D., Gustafsson, Ö., 2016. Sources of black carbon to the Himalayan–Tibetan Plateau glaciers. *Nat. Commun.* 7, 12574.
- Li, C.L., Han, X.W., Kang, S.C., Yan, F.P., Chen, P.F., Hu, Z.F., Yang, J.H., Ciren, D.J., Gao, S.P., Sillanpaa, M., Han, Y.M., Cui, Y.Y., Liu, S., Smith, K.R., 2019. Heavy near-surface PM_{2.5} pollution in Lhasa, China during a relatively static winter period. *Chemosphere* 214, 314–318.
- Liu, X., Shen, G., Chen, L., Qian, Z., Zhang, N., Chen, Y., Chen, Y., Cao, J., Cheng, H., Du, W., Li, B., Li, G., Li, Y., Liang, X., Liu, M., Lu, H., Luo, Z., Ren, Y., Zhang, Y., Zhu, D., Tao, S., 2021. Spatially resolved emission factors to reduce uncertainties in air pollutant emission estimates from the residential sector. *Environ. Sci. Technol.* 55, 4483–4493.
- Liu, K., Wu, Q., Ren, Y., Wang, S., 2022. Air pollutant emissions from residential solid fuel combustion in the Pan-third pole region. *Environ. Sci. Technol.* 56, 15347–15355.
- Lu, Z., Zhang, Q., Streets, D.G., 2011. Sulfur dioxide and primary carbonaceous aerosol emissions in China and India, 1996–2010. *Atmos. Chem. Phys.* 11, 9839–9864.
- Lu, X., Zhang, S.J., Xing, J., Wang, Y.J., Chen, W.H., Ding, D., Wu, Y., Wang, S.X., Duan, L., Hao, J.M., 2020. Progress of air pollution control in China and its challenges and opportunities in the ecological civilization era. *Engineering* 6, 1423–1431.
- Luo, J.M., Han, Y.M., Zhao, Y., Liu, X.R., Huang, Y.F., Wang, L.F., Chen, K.J., Tao, S., Liu, J.F., Ma, J.M., 2020. An inter-comparative evaluation of PKU-FUEL global SO₂ emission inventory. *Sci. Total Environ.* 722.
- Ni, K., Carter, E., Schauer, J.J., Ezzati, M., Zhang, Y.X., Niu, H.J., Lai, A.M., Shan, M., Wang, Y.Q., Yang, X.D., Baumgartner, J., 2016. Seasonal variation in outdoor, indoor, and personal air pollution exposures of women using wood stoves in the Tibetan Plateau: baseline assessment for an energy intervention study. *Environ. Int.* 94, 449–457.
- O'Neill, B.C., Tebaldi, C., van Vuuren, D.P., Eyring, V., Friedlingstein, P., Hurtt, G., Knutti, R., Kriegler, E., Lamarque, J.F., Lowe, J., Meehl, G.A., Moss, R., Riahi, K., Sanderson, B.M., 2016. The scenario model intercomparison project (ScenarioMIP) for CMIP6. *Geosci. Model Dev.* 9, 3461–3482.
- Popp, A., Calvin, K., Fujimori, S., Havlik, P., Humpenoder, F., Stehfest, E., Bodirsky, B.L., Dietrich, J.P., Doelman, J.C., Gusti, M., Hasegawa, T., Kyle, P., Obersteiner, M., Tabeau, A., Takahashi, K., Valin, H., Waldhoff, S., Weindl, I., Wise, M., Kriegler, E., Lotze-Campen, H., Fricko, O., Riahi, K., van Vuuren, D.P., 2017. Land-use futures in the shared socio-economic pathways. *Glob. Environ. Chang.* 42, 331–345.
- Ran, L., Lin, W.L., Deji, Y.Z., La, B., Tsering, P.M., Xu, X.B., Wang, W., 2014. Surface gas pollutants in Lhasa, a highland city of Tibet – current levels and pollution implications. *Atmos. Chem. Phys.* 14, 10721–10730.
- Rao, S., Klimont, Z., Smith, S.J., Van Dingenen, R., Dentener, F., Bouwman, L., Riahi, K., Amann, M., Bodirsky, B.L., van Vuuren, D.P., Aleluia Reis, L., Calvin, K., Drouet, L., Fricko, O., Fujimori, S., Gernaat, D., Havlik, P., Harmsen, M., Hasegawa, T., Heyes, C., Hilaire, J., Luderer, G., Masui, T., Stehfest, E., Strefler, J., van der Sluis, S., Tavoni, M., 2017. Future air pollution in the shared socio-economic pathways. *Glob. Environ. Chang.* 42, 346–358.
- Riahi, K., van Vuuren, D.P., Kriegler, E., Edmonds, J., O'Neill, B.C., Fujimori, S., Bauer, N., Calvin, K., Dellink, R., Fricko, O., Lutz, W., Popp, A., Cuaresma, J.C., Kc, S., Leimbach, M., Jiang, L., Kram, T., Rao, S., Emmerling, J., Ebi, K., Hasegawa, T., Havlik, P., Humpenöder, F., Da Silva, L.A., Smith, S., Stehfest, E., Bosetti, V., Eom, J., Gernaat, D., Masui, T., Rogelj, J., Strefler, J., Drouet, L., Krey, V., Luderer, G., Harmsen, M., Takahashi, K., Baum stark, L., Doelman, J.C., Kainuma, M., Klimont, Z., Marangoni, G., Lotze-Campen, H., Obersteiner, M., Tabeau, A., Tavoni, M., 2017. The shared socioeconomic pathways and their energy, land use, and greenhouse gas emissions implications: an overview. *Glob. Environ. Chang.* 42, 153–168.
- Rogelj, J., Popp, A., Calvin, K.V., Luderer, G., Emmerling, J., Gernaat, D., Fujimori, S., Strefler, J., Hasegawa, T., Marangoni, G., Krey, V., Kriegler, E., Riahi, K., van Vuuren, D.P., Doelman, J., Drouet, L., Edmonds, J., Fricko, O., Harmsen, M., Havlik, P., Humpenöder, F., Stehfest, E., Tavoni, M., 2018. Scenarios towards limiting global mean temperature increase below 1.5 °C. *Nat. Clim. Chang.* 8, 325–332.
- Scholze, M., Knorr, W., Arnell, N.W., Prentice, I.C., 2006. A climate-change risk analysis for world ecosystems. *Proc. Natl. Acad. Sci.* 103, 13116–13120.
- Shen, G., Du, W., Luo, Z., Li, Y., Cai, G., Lu, C., Qiu, Y., Chen, Y., Cheng, H., Tao, S., 2020. Fugitive emissions of CO and PM_{2.5} from indoor biomass burning in chimney stoves based on a newly developed carbon balance approach. *Environ. Sci. Technol. Lett.* 7, 128–134.
- Shen, G.F., Ru, M.Y., Du, W., Zhu, X., Zhong, Q.R., Chen, Y.L., Shen, H.Z., Yun, X., Meng, W.J., Liu, J.F., Cheng, H.F., Hu, J.Y., Guan, D.B., Tao, S., 2019. Impacts of air pollutants from rural Chinese households under the rapid residential energy transition. *Nat. Commun.* 10, 3405.
- Sierra-Hernández, M.R., Beaudon, E., Gabrielli, P., Thompson, L., 2019. 21st-century Asian air pollution impacts glacier in northwestern Tibet. *Atmos. Chem. Phys.* 19, 15533–15544.
- Tao, S., Ru, M.Y., Du, W., Zhu, X., Zhong, Q.R., Li, B.G., Shen, G.F., Pan, X.L., Meng, W.J., Chen, Y.L., Shen, H.Z., Lin, N., Su, S., Zhuo, S.J., Huang, T.B., Xu, Y., Yun, X., Liu, J., F., Wang, X.L., Liu, W.X., Cheng, H.F., Zhu, D.Q., 2018. Quantifying the rural residential energy transition in China from 1992 to 2012 through a representative national survey. *Nat. Energy* 3, 567–573.
- Tong, D., Cheng, J., Liu, Y., Yu, S., Yan, L., Hong, C., Qin, Y., Zhao, H., Zheng, Y., Geng, G., Li, M., Liu, F., Zhang, Y., Zheng, B., Clarke, L., Zhang, Q., 2020. Dynamic projection of anthropogenic emissions in China: methodology and 2015–2050 emission pathways under a range of socio-economic, climate policy, and pollution control scenarios. *Atmos. Chem. Phys.* 20, 5729–5757.
- van Vuuren, D.P., Lucas, P.L., Hilderink, H., 2007. Downscaling drivers of global environmental change: enabling use of global SRES scenarios at the national and grid levels. *Glob. Environ. Chang.* 17, 114–130.
- Van Vuuren, D.P., Edmonds, J., Kainuma, M., Riahi, K., Thomson, A., Hibbard, K., Hurtt, G.C., Kram, T., Krey, V., Lamarque, J.-F., Masui, T., Meinshausen, M., Nakicenovic, N., Smith, S.J., Rose, S.K., 2011. The representative concentration pathways: an overview. *Clim. Chang.* 109, 5–31.
- van Vuuren, D.P., Stehfest, E., Gernaat, D.E.H.J., Doelman, J.C., van den Berg, M., Harmsen, M., de Boer, H.S., Bouwman, L.F., Daioglou, V., Edelenbosch, O.Y., Girod, B., Kram, T., Lassaletta, L., Lucas, P.L., van Meijl, H., Müller, C., van Ruijen, B.J., van der Sluis, S., Tabeau, A., 2017. Energy, land-use and greenhouse gas emissions trajectories under a green growth paradigm. *Glob. Environ. Chang.* 42, 237–250.
- Wang, R., Tao, S., Balkanski, Y., Ciais, P., Boucher, O., Liu, J., Piao, S., Shen, H., Vuolo, M.R., Valari, M., Chen, H., Chen, Y., Cozic, A., Huang, Y., Li, B., Li, W., Shen, G., Wang, B., Zhang, Y., 2014. Exposure to ambient black carbon derived from a unique inventory and high-resolution model. *Proc. Natl. Acad. Sci.* 111, 2459–2463.
- Wu, B., Shen, X., Cao, X., Yao, Z., Wu, Y., 2016. Characterization of the chemical composition of PM_{2.5} emitted from on-road China III and China IV diesel trucks in Beijing, China. *Sci. Total Environ.* 551–552, 579–589.
- Wu, J., Lu, J., Min, X., Zhang, Z., 2018. Distribution and health risks of aerosol black carbon in a representative city of the Qinghai-Tibet Plateau. *Environ. Sci. Pollut. Res.* 25, 19403–19412.
- Xu, H., Ren, Y.A., Zhang, W., Meng, W., Yun, X., Yu, X., Li, J., Zhang, Y., Shen, G., Ma, J., Li, B., Cheng, H., Wang, X., Wan, Y., Tao, S., 2021. Updated global black carbon emissions from 1960 to 2017: improvements, trends, and drivers. *Environ. Sci. Technol.* 55, 7869–7879.
- Yang, S., Xu, B., Cao, J., Zender, C.S., Wang, M., 2015. Climate effect of black carbon aerosol in a Tibetan Plateau glacier. *Atmos. Environ.* 111, 71–78.
- Yang, J., Kang, S., Ji, Z., 2020. Critical contribution of south Asian residential emissions to atmospheric black carbon over the Tibetan plateau. *Sci. Total Environ.* 709, 135923.
- Yang, J.H., Ji, Z.M., Kang, S.C., Tripathee, L., 2021. Contribution of South Asian biomass burning to black carbon over the Tibetan Plateau and its climatic impact. *Environ. Pollut.* 270.